

Crashworthiness of Glass/Polyester Composite Tubular Structures

S. Solaimurugan^a and R.Velmurugan^b

^aDept. of Mechanical Engg., Fatima Michael College of Engg. and Tech., Madurai, Tamilnadu, India
Email: solaimuruganiitm@yahoo.com

^bDept. of Aerospace Engg., Indian Institute of Technology Madras, Chennai, Tamilnadu, India
Corresponding Author, Email: rvel@iitm.ac.in

ABSTRACT:

Advances in automotive and aircraft sectors lead to production of very high speed vehicles. The amount of energy that a vehicle absorbs during collision is a concern to ensure safer and more reliable vehicles. The FRP composite structural members dissipate huge amount of energy during collision and improves the vehicle crashworthiness. Thin walled FRP composite cylindrical shells are used as energy absorbers and absorb large amount of impact energy during collision. The energy absorbing capability of thin walled composite shells is quantified by specific energy absorption (SEA), the energy absorbed per unit mass of crushed material. The SEA of composite shells depends on the way in which the tube material is crushed (axially or laterally). Progressive deformation and stable collapse significantly reduce the forces experienced by the passengers in the event of sudden collision. This paper investigates the influence of fibre orientation and stacking sequence on the SEA of six-ply, 0°/90° Glass/Polyester composite cylindrical shells under axial and lateral compression. The crushing resistance and SEA vary with proportion of axial (0°) and hoop (90°) fibre content and stacking sequence in the tubes. The energy absorption capability under lateral crushing is compared with that of axial compression.

KEYWORDS:

Composite tubes; Crashworthiness; Fracture toughness; Delamination; Progressive crushing

CITATION:

S. Solaimurugan and R.Velmurugan. 2015. Crashworthiness of Glass/Polyester Composite Tubular Structures, *Int. J. Vehicle Structures & Systems*, 7(3), 118-122. doi:10.4273/ijvss.7.3.06.

ACRONYMS AND NOMENCLATURE:

WRM	Woven roving glass fibre material
UD	Unidirectional glass fibre material
SEA	Specific Energy Absorption (J/kg)
G_{Ic}	Mode I interlaminar fracture toughness (kJ/m^2)
h	Stroke length for axial crushing of cylindrical shell
U_d	Energy required for circumferential delamination (J)
U_a	Energy req'd for petal formation (axial cracks) (J)
U_b	Energy required for bending of petals (J)
U_f	Energy dissipated due to friction between crushing platen and petals (J)
W_e	External work done by applied force P (J)
K_I	Mode I stress intensity factor
E	Young's modulus (Pa)
n	Number of petals
σ	Circumferential stress (MPa)
σ_u	Fracture strength in uni-axial tension (MPa)
σ_b	Flexural strength (MPa)
σ_s	Interlaminar short beam shear strength (MPa)
θ	Bending angle of petals
μ	Coeff. of friction between petal & crushing platen
D, r	Diameter and radius of cylindrical shell (mm)
H, t	Height and thickness of cylindrical shell (mm)

1. Introduction

Advanced technologies in automotive and aircraft sectors lead to production of very high speed vehicles. However, the amount of energy that a vehicle absorbs during collision is a matter of concern to ensure safer and more reliable vehicles, because passenger's safety is

the prominent requirement. The FRP composite structural members dissipate huge amount of energy during collision and improves the vehicle crashworthiness. Thin walled composite cylindrical tubes are common structural components that can be used for a wide variety of applications including drive shafts, chassis of automobiles and trusses for space vehicles. They offer the stiffness of conventional metals at lower weight and are used as energy absorbers [1-3]. FRP composite bumper beam is one of the main components of car that protect passengers from front and rear collision [4]. The energy absorbing capability of FRP composite cylindrical tubes used as energy absorbers, by destroying itself progressively, depends on the way in which the tube material is crushed. The shell which collapses in a stable, progressive and controlled manner can dissipate large amount of energy [2, 3, 5-9]. Progressive deformation and stable collapse significantly reduce the forces experienced by the passengers in the event of sudden collision [10].

In this investigation the influence of fibre orientation on energy absorbing capability of 0°/90° glass/polyester composite cylindrical structures having various proportions axial (0°) and circumferential (90°) fibres are studied under axial and lateral crushing. An analytical model is developed based on energy approach to predetermine the steady state mean crush load of cylindrical composite shells under axial compression. The model results are validated by experimental results,

and show good agreement. The proportions of energy dissipated through various failure modes under axial compression are analyzed. The energy absorption capability under lateral crushing is compared with that of axial compression.

2. Composite tubular specimens

Series of six-ply cylindrical tubes having cross ply fibre orientations (fibres are oriented along the axial and hoop directions only) are prepared with woven roving (WRM), unidirectional (UD) glass fibre mats and polyester resin. Cylindrical preforms have WRM mats as outer and inner most layer of the tube wall, and the UD materials are placed in between [WRM/(UD)₄/WRM]. The stacking sequence is from outer to inner radius of the tubular structure. WRM is aligned such that fibres are being oriented along the axial and hoop directions. Tubes are made with 14.5, 50, 67.8 and 85.5 % of axial (0°) fibres; the remaining fibres being oriented along the circumferential (90°) direction. Fig. 1 shows the tubular specimens of length around 160 mm for axial crushing and 65 mm for lateral crushing are cut. The inner diameters of the tube is 63.5mm. For axial crushing, one end of the specimen is chamfered while the other end being flat. For lateral crushing, both ends are flat.



Fig. 1: Specimens for axial (left) and lateral (right) crushing

3. Analytical modeling

When the composite tubular specimen is crushed axially, the circumferential delamination takes place in the middle of the thickness. Delaminated layers are strained circumferentially and the cracks are formed in the axial direction. Due to these circumferential delamination and axial crack, petals are formed. Schematic diagram of crush zone is shown in Fig. 2. Crushing is progressed towards other end of tube through bending of petals away from the centre of the wall thickness, which are broken at the root of petal. Brittleness of composite tube material causes the crush zone to progress through successive cycles with stroke length, *h*. The idealized model of the crush zone is shown in Fig. 3. The energy terms assumed to be involved in the crush zone of axially crushed tube are:

- External work done by the crushing platen (*W_e*).
- Energy dissipated during circumferential delamination (*U_d*).
- Energy dissipated during petal formation (axial cracks) (*U_a*).

- Energy dissipated on bending of petals (*U_b*).
- Energy dissipated through interlaminar shear deformation in the petals during bending (*U_s*).
- Energy dissipated due to friction between crushing platen and petals (*U_f*).

The mode I interlaminar fracture toughness, *G_{IC}* are experimentally studied, and these values are used for energy calculations. The work done on the specimen is dissipated through the remaining five energy terms.

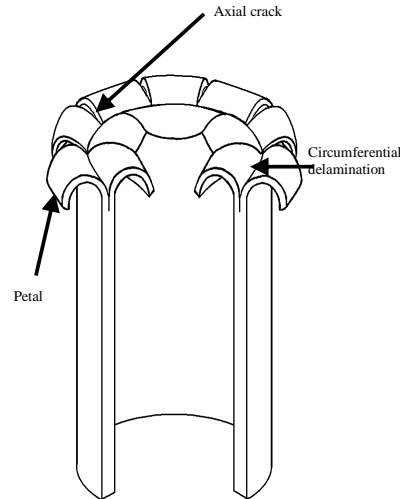


Fig. 2: Schematic of crush zone for axial crush

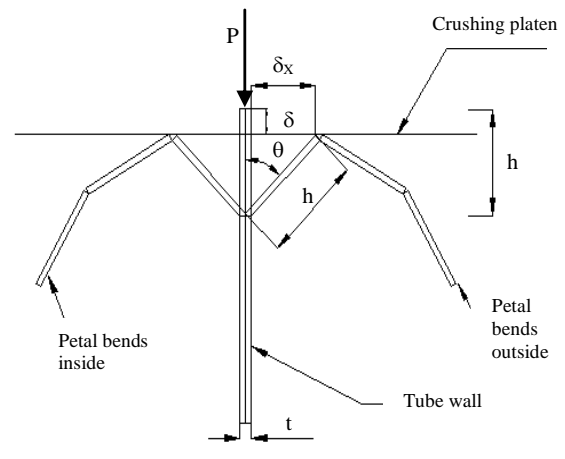


Fig. 3: Idealised model of crush zone

The work done by external load, *P* on the crushing displacement, δ is given by,

$$W_e = P\delta = P(h - h\cos\theta) \tag{1}$$

The energy released through delamination to occur circumferentially in a single stroke is given by,

$$U_d = G_{IC} 2\pi r h \tag{2}$$

Where *G_{IC}* is the critical strain energy release rate per unit interlaminar delaminated crack area and *h* is the crack length for single stroke. *G_{IC}* is determined experimentally through DCB test [7].

According to Griffith energy criterion for fracture state, crack growth can occur if the energy required to form the additional crack surfaces (*G*) can just be delivered by the system as a release of strain energy. The

G_I for in-plane mode I failure resulting axial cracks is given by,

$$G_I = K_I^2 / E \quad (3a)$$

where K_I is the mode I stress intensity factor.

For the linear crack of any number of petals, K_I is approximated [11] as,

$$K_I = \sigma \sqrt{\pi h} F(n) \quad (3b)$$

Where $F(n) = 2/\sqrt{n}$ is a function of number of petals, n and σ is the circumferential stress. As discussed earlier the material splaying outwards flares into petals, and the material splaying inwards just bends without petalling. So, the total axial crack area is $A = thn$. Where, t is the thickness of tube wall. Therefore, the total energy required for the formation of axial cracks is given by,

$$U_a = \frac{\pi h \sigma^2}{E} \left(\frac{2}{\sqrt{n}} \right)^2 thn \quad (4)$$

Though the axial cracks are initiated by local buckling of the chamfered portion in the tube under axial compression, the axial cracks are propagated due to the tensile hoop stress in the progressive crush zone. Since this analytical model is focused on the steady state progressive crush zone, it is assumed that the failure stress due to the circumferential strain is equal to the ultimate fracture strength in uni-axial tension (σ_u). Therefore the tensile strength values of the planar specimens are used in the model for estimating the energy released through petal formation (axial cracking). The series of three-ply laminates provide strength values [6] of material in the outer and inner half of the tube thickness, which are flaring outwards and inwards in the six-ply tubes, respectively. The corresponding strength values of outer and inner half of the tube thickness are substituted in the analytical expression. At fracture $\sigma = \sigma_u$, thus

$$U_a = 4\sigma_u^2 \pi h^2 t / E \quad (5)$$

The value of E is calculated from linear stress strain relation $E = \sigma_u / \varepsilon = \sigma_u r / (h \sin \theta)$. Thus, the total energy required for petal formation, U_a , is given by,

$$U_a = 4\sigma_u \pi h^3 t \sin \theta / r \quad (6)$$

Petals with length equal to axial crack length of single cycle, h are formed during axial crushing, and are assumed as cantilever beams of constant thickness and rectangular shape at each stage of crack propagation. The fixed portion of this beam is broken by bending at the end of every cycle, and the circumferential delamination followed by axial cracks propagates for next cycle. The fully plastic state bending moment per unit width $M_b = \sigma_y t_{petal}^2 / 4$ is used for calculating the petal bending work in case of metallic tubes, where σ_y is bending yield strength [12]. Here, the fracture state bending moment per unit width $M_b = \sigma_b t_{petal}^2 / 4$ is used for calculating petal bending work for thermoset glass/polyester composites, where σ_b is the flexural

strength. Energy required for breaking the petals by bending both inside and outside of the wall is given by,

$$U_b = \int_0^{\pi/2} \frac{\sigma_b b t^2}{8} d\theta = \frac{\pi \sigma_b b t^2}{16} \quad (7)$$

Where, b is the total width of petals ($b=2\pi r$) and θ is the bending angle of petals. This energy is maximum when θ is equal to 90° .

The energy dissipated by the shear deformation of the matrix material between layers due to bending of petals of length h (length of crush zone) is given by,

$$\begin{aligned} dU_s &= \int \sigma_s \varepsilon dV \\ \varepsilon &= \delta_x / h \\ U_s &= \int_0^{\pi/2} \sigma_s \left(\frac{h \sin \theta}{h} \right) (2\pi r t h) d\theta = \int_0^{\pi/2} 2\pi r t \sigma_s \sin \theta d\theta \end{aligned} \quad (8)$$

Where σ_s is the interlaminar short beam shear strength and $\delta_x = h \sin \theta$.

The debris inside the circumferential delamination crack and petals are rubbing on the crushing platen during the progression of crush zone. The energy dissipated due to friction between the petals that flare both inside and outside the tube wall and the crushing platen [13] is given by,

$$U_f = 2\mu P \delta_x \quad (9)$$

Where $\delta_x = h \sin \theta$. The coefficient of friction between petal and crushing platen, μ is equal to approximately 0.35 [14].

According to the balance of energy, the work done on the specimen is equal to the sum of energy dissipated by the specimen,

$$\begin{aligned} W_e &= U_d + U_a + U_b + U_s + U_f \\ P(\delta - 2\mu\delta_x) &= G_{lc} 2\pi r h + 4\sigma_u \pi h^3 t \sin \theta / r \\ &+ \int_0^{\pi/2} \frac{\sigma_b b t^2}{8} d\theta + \int_0^{\pi/2} 2\pi r t \sigma_s \sin \theta d\theta \end{aligned} \quad (10)$$

The energy terms related to external work, frictional work, circumferential delamination work, interlaminar shear work and petal bending work are maximum when bending angle θ is equal to 90° . The thickness and diameter of cylindrical shell is constant throughout the length of specimen, and hence the crush load oscillates in a regular way in the stable controlled progressive crush zone, and the average load per wave is same throughout the stable crush length of specimen. So the integrated four terms are added as follows,

$$P = \frac{1}{h(1-2\mu)} \left(G_{lc} 2\pi r h + 4\sigma_u \pi h^3 t \sin \theta / r + \pi \sigma_b b t^2 / 16 + 2\pi r t \sigma_s \right) \quad (11)$$

The expression for θ in the energy term related to axial crack is obtained by equating circumferential strain to the fracture strain in uni-axial tension, ε_f . Thus $\sin \theta = \varepsilon_f r / h$. Minimization of load P in Eqn.(11), i.e., $\partial P / \partial h = 0$, leads to,

$$h = (r^2 t \theta / 32 \sin \theta)^{1/3} \quad (12)$$

The mean crush load of cylindrical shells under axial compression are predetermined by incorporating the values of G_{Ic} , σ_u , σ_b and σ_s from our recent article [15], and h obtained through iteration from Eqn. (12) in the energy balance Eqn. (11).

4. Results and discussion

Quasi-static tube crush is the representative test which provides the correct overall trend that is experienced by a composite member during a crash. Hence the tubular specimens were subjected to axial and lateral compression in the UTM with a crosshead speed of 2 mm/min. Three samples of each tube were tested. The tested specimens in axial and lateral crushing alongwith load-crush displacement curves are shown in Figs. 4&6 and Figs. 5&7, respectively. In case of axial crushing, the load increases with crushing displacement upto a peak value and reaches the plateau state with mild load oscillation following a small drop in load. In the lateral crushing, load increases with crushing displacement upto a peak value and then gradually reduces. As the initial slope of load-displacement curve for axial crushing depends on the chamfer angle, mean crush load is calculated in the steady state crush zone.

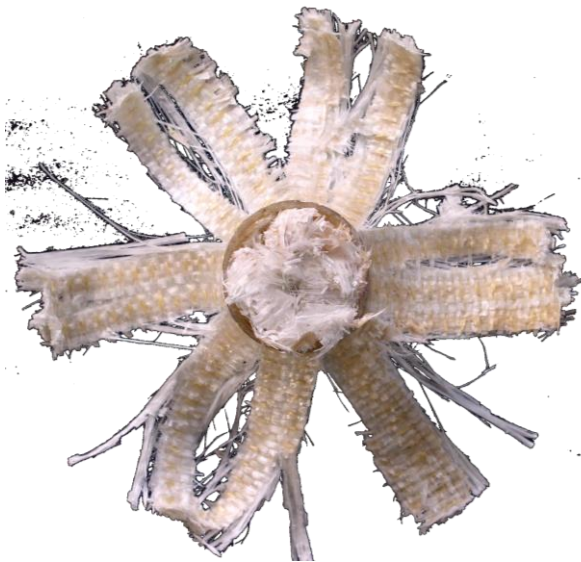


Fig. 4: Tested specimen - Axial crushing



Fig. 5: Tested specimen - Lateral crushing

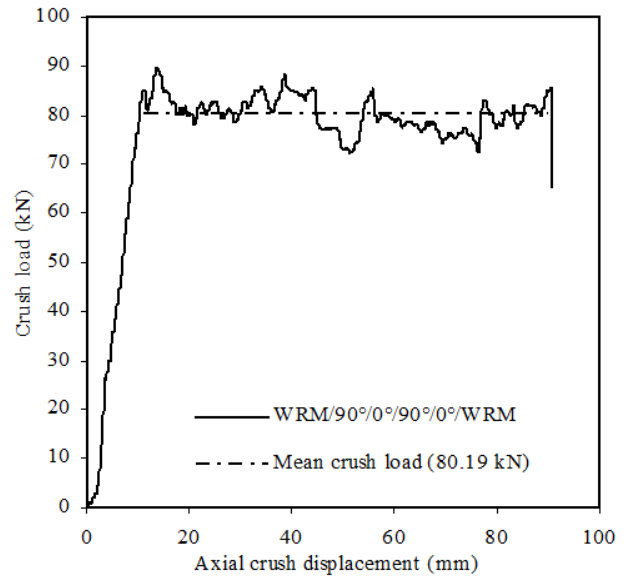


Fig. 6: Load vs. Crush displacement - Axial crushing

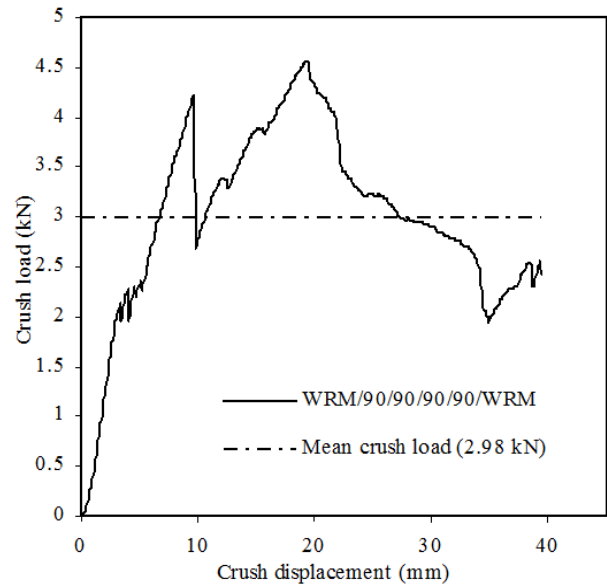


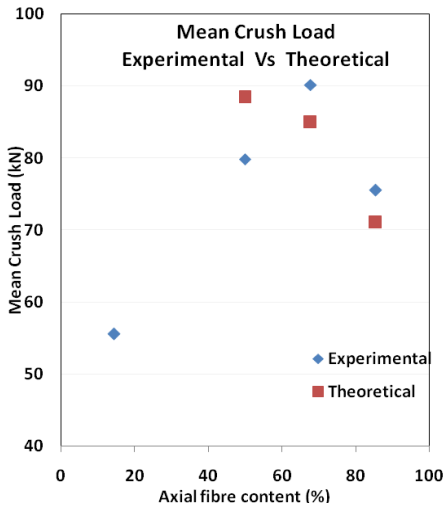
Fig. 7: Load vs. Crush displacement - Lateral crushing

Specific energy absorption, SEA is calculated as energy absorbed per unit mass of the tube material crushed, and the values are reported in Table 1. Higher SEA is observed when the tubes are crushed progressively. In the tubes undergo progressive crushing under axial compression, presence of axial fibers close to inner surface and the proper proportion of circumferential fibres close to outer surface of the tube wall lead to higher energy dissipation. Because the axial fibres placed near the inner surface offer more resistance to bending of petals inside the tube, and the hoop fibres placed near the outer surface offers higher resistance to axial cracking, however much amount of hoop fibres avoids the event of progressive crushing. In the case of axial crushing, SEA increases with increasing proportion of axial fibre content upto certain limit (68% of 0° fibres) above which SEA decreases. But in the case of lateral crushing, SEA decreases with increasing proportion of axial fibre content. Also it is observed that SEA of tubes under lateral crushing is much less comparing to axial crushing.

Table 1: SEA of cylindrical shells

Stacking sequence	Axial (0°) fibre content (%)	Wall thick (mm)	Crushing SEA (J/kg)	
			Axial	Lateral
WRM/(90) ₄ /WRM	14.5	4.4	31740	1220
WRM/(90/0) ₂ /WRM	50.0	4.4	43040	990
WRM/90/(0) ₃ /WRM	67.8	4.2	50480	630
WRM/(0) ₄ /WRM	85.5	4.2	45350	210

The mean crush load of composite cylindrical shells under axial compression are pre-determined from the analytical model developed based on energy approach. The experimental results are used for validation of analytical model results. Fig. 8 shows good agreement between experimental results and analytical model results. This model is valid only for tubes that undergo stable progressive crushing through the formation of petals during axial compression. It is observed from Eqn.(4) that energy dissipated through axial crack formation, U_a depends on the tensile hoop strength of layers placed in the outer half of the tube wall thickness, which are higher for circumferential fibres. Through proper stacking sequence the energy dissipated by axial crack propagation is improved for single stroke length.

**Fig. 8: Mean crush load - Experimental vs. Theoretical**

5. Conclusions

Higher SEA is observed when the tubes are crushed progressively in both axial and lateral crushing. In the case of axial crushing, SEA increases with increasing proportion of axial fibre content upto certain limit (68% of 0° fibres) above which SEA decreases. Whereas in the case of lateral crushing, SEA increases with increasing proportion of hoop (90°) fibre content. The hoop fibres placed near the inner surface offer higher resistance to lateral crushing comparing to near the outer surface. Also it is observed that SEA of tubes under lateral crushing is much less comparing to axial crushing.

REFERENCES:

[1] G.L. Farley. 1991. The effects of crushing speed on the energy absorption capability of composite tubes, *J. Composite Materials*, 25, 1314-1329.

[2] D. Hull. 1991. A unified approach to progressive crushing of fibre-reinforced composite tubes, *Composite Science Tech.*, 40, 377-421. [http://dx.doi.org/10.1016/0266-3538\(91\)90031-J](http://dx.doi.org/10.1016/0266-3538(91)90031-J).

[3] A.G. Mamalis, M. Robinson, D.E. Manolakos, G.A. Demosthenous, M.B. Ioannidis and J. Carruthers. 1997. Crashworthy capability of composite material structures, *Composite Structures*, 37(2), 109-134. [http://dx.doi.org/10.1016/S0263-8223\(97\)80005-0](http://dx.doi.org/10.1016/S0263-8223(97)80005-0).

[4] R. Hosseinzadeh, M.M. Shokrieh and L.B. Lessard. 2005. Parametric study of automotive composite bumper beams subjected to low-velocity impacts, *Composite Structures*, 68(4), 419-427. <http://dx.doi.org/10.1016/j.compstruct.2004.04.008>.

[5] R. Velmurugan, N.K. Gupta, S. Solaimurugan and A. Elayaperumal. 2004. The effect of stitching on FRP cylindrical shells under axial compression, *Int. J. Impact Engineering*, 30(8-9), 923-938. <http://dx.doi.org/10.1016/j.ijimpeng.2004.04.007>.

[6] S. Solaimurugan and R. Velmurugan. 2007. Progressive crushing of stitched glass/polyester composite cylindrical shells, *Composites Science and Tech.*, 67(3-4), 422-437. <http://dx.doi.org/10.1016/j.compscitech.2006.09.002>.

[7] S. Solaimurugan and R. Velmurugan. 2007. Influence of fibre orientation and stacking sequence on petalling of glass/polyester composite cylindrical shells under axial compression, *Int. J. Solids and Structures*, 44, 6999-7020. <http://dx.doi.org/10.1016/j.ijsolstr.2007.03.025>.

[8] C. Bisagni, G. Di Pietro, L. Frascini and D. Terletti. 2005. Progressive crushing of fibre-reinforced composite structural components of a Formula One racing car, *Composite Structures*, 68(4), 491-503. <http://dx.doi.org/10.1016/j.compstruct.2004.04.015>.

[9] A.G. Mamalis, D.E. Manolakos, M.B. Ioannidis and D.P. Papapostolou. 2006. The static and dynamic axial collapse of CFRP square tubes: Finite element modeling, *Composite Structures*, 74(2), 213-225. <http://dx.doi.org/10.1016/j.compstruct.2005.04.006>.

[10] A.G. Mamalis, D.E. Manolakos, M.B. Ioannidis and D.P. Papapostolou. 2004. Crashworthy characteristics of axially statically compressed thin-walled square CFRP composite tubes: experimental, *Composite Structures*, 63(3-4), 347-360. [http://dx.doi.org/10.1016/S0263-8223\(03\)00183-1](http://dx.doi.org/10.1016/S0263-8223(03)00183-1).

[11] B. Landkof and W. Goldsmith. 1985. Petalling of thin, metallic plates during penetration by cylindro-conical projectiles, *Int. J. Solids Structures*, 21(3), 245-266. [http://dx.doi.org/10.1016/0020-7683\(85\)90021-6](http://dx.doi.org/10.1016/0020-7683(85)90021-6).

[12] T.Y. Reddy and S.R. Reid. 1986. Axial splitting of circular metal tubes, *Int. J. Mech. Sciences*, 28(2), 111-131. [http://dx.doi.org/10.1016/0020-7403\(86\)90018-4](http://dx.doi.org/10.1016/0020-7403(86)90018-4).

[13] W.H. Tao, R.E. Robertson and P.H. Thornton. 1993. Effects of material properties and crush conditions on the crush energy absorption of fiber composite rods, *Composites Science and Technology*, 47(4), 405-418. [http://dx.doi.org/10.1016/0266-3538\(93\)90009-6](http://dx.doi.org/10.1016/0266-3538(93)90009-6).

[14] N.K. Gupta, R. Velmurugan and S.K. Gupta. 1997. An analysis of axial crushing of composite tubes, *J. Composite Materials*, 31(13), 1262-1286. <http://dx.doi.org/10.1177/002199839703101301>.

[15] S. Solaimurugan and R. Velmurugan. 2008. Influence of in-plane fibre orientation on mode I interlaminar fracture toughness of stitched glass/polyester composites, *Composites Science and Technology*, 68, 1742-1752. <http://dx.doi.org/10.1016/j.compscitech.2008.02.008>.